

## RMC modelling of the structure of expanded liquid mercury along the co-existence curve

This article has been downloaded from IOPscience. Please scroll down to see the full text article.

1998 J. Phys.: Condens. Matter 10 9221

(<http://iopscience.iop.org/0953-8984/10/41/005>)

View [the table of contents for this issue](#), or go to the [journal homepage](#) for more

Download details:

IP Address: 171.66.16.210

The article was downloaded on 14/05/2010 at 17:32

Please note that [terms and conditions apply](#).

## RMC modelling of the structure of expanded liquid mercury along the co-existence curve

T Arai<sup>†</sup> and R L McGreevy<sup>‡</sup>

<sup>†</sup> National Defense Academy, Department of Mathematics and Physics, Yokosuka 239, Japan

<sup>‡</sup> Studsvik Neutron Research Laboratory, S-611 82 Nyköping, Sweden

Received 21 May 1998, in final form 4 August 1998

**Abstract.** The structure factors of liquid Hg at 13 temperatures/pressures along the liquid–vapour co-existence curve have been modelled using the reverse Monte Carlo (RMC) method. The resulting configurations are consistent with the idea that the liquid contains atoms which can be considered as being in a ‘metallic’ environment, characterized by a larger number of near neighbours at a relatively short distance, and atoms which are in a ‘semiconducting’ environment, characterized by a smaller number of neighbours at a slightly longer distance. As the temperature increases and the density decreases, the proportion of ‘metallic’ atoms decreases. The metal–non-metal transition at  $\rho_{M-NM} \approx 9 \text{ g cm}^{-3}$  ( $0.027 \text{ \AA}^{-3}$ ) may be considered as a percolation transition in the metallic bond network. At lower densities the metal atoms occur in isolated clusters, and there is some evidence that the critical point at  $\rho_c = 5.8 \text{ g cm}^{-3}$  ( $0.0174 \text{ \AA}^{-3}$ ) coincides with the disappearance of these clusters.

### 1. Introduction

The density of liquid mercury at ambient temperature and pressure is  $0.0407 \text{ \AA}^{-3}$ . Various experimental results have shown that along the liquid–vapour coexistence curve there is a metal–non-metal (M–NM) transition at an atomic number density  $\rho_{M-NM} \approx 0.027 \text{ \AA}^{-3}$ , which is significantly higher than the critical point density  $\rho_c = 0.0174 \text{ \AA}^{-3}$ . Much experimental effort has been devoted to measuring physical properties near these two points [1–5] and much theoretical effort to explaining them [6–8]. Obviously, it is important to have some understanding of any possible structural changes, but unfortunately computer simulation methods such as molecular dynamics are difficult to apply since the interatomic potential required is complex even at ambient temperature and changes as temperature increases, particularly of course in the region of the transitions of interest.

Previously we have reported on the application of reverse Monte Carlo (RMC) modelling and ‘atom removal’ methods to the study of the structure of expanded liquid Cs [9–11]. The advantage of RMC methods is that no interatomic potential is required—a three-dimensional model of the atomic structure is obtained on the basis of diffraction data. The structure is not unique, but it can nevertheless provide a great deal of insight into the type of structural changes that occur as the liquid density decreases. In the case of Cs it was possible to characterize the M–NM transition as a sort of metallic bonding percolation transition and to suggest that the changes in potential at this point probably determined the critical point, rather than *vice versa*.

Tamura [5] has measured the structure factor of liquid Hg at 13 temperatures/pressures near the co-existence curve from room temperature to near the critical point,  $T_c$ , using energy

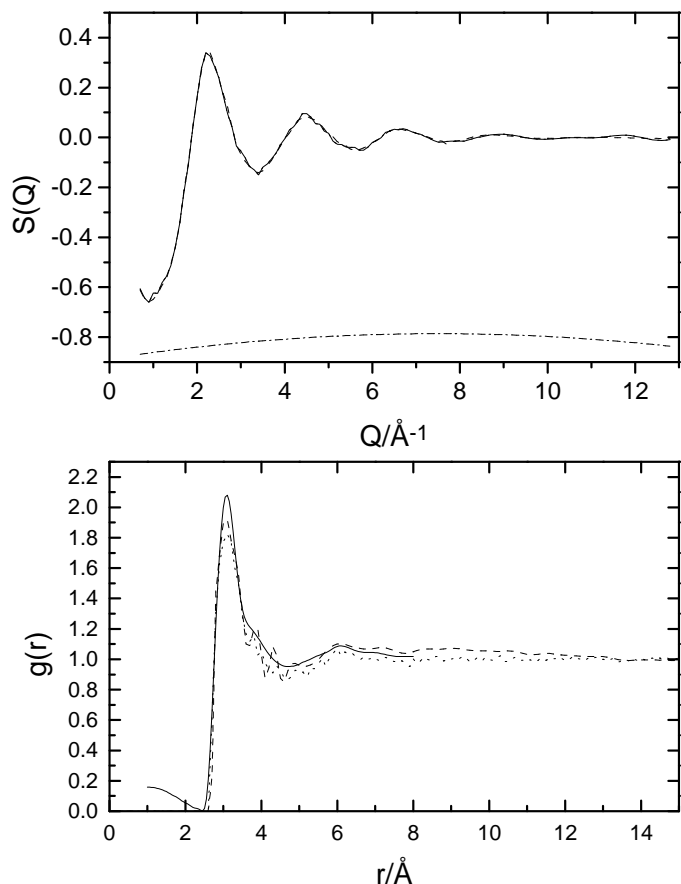


**Figure 1.** Structure factor,  $S(Q)$ , and radial distribution function,  $g(r)$ , from experiment at 1803 K [5] (full curve), MCGR fit (dashed curve) and RMC fit to the MCGR fit (dotted curve). The dash-dotted curve is the background correction from the MCGR fit, multiplied by 10 and shifted by  $-0.8$  for clarity. See the text for further details.

dispersive x-ray diffraction. The structure factor,  $S(Q)$ , in common with many other metals in groups IIB–IVA of the periodic table, such as Ga and Tl, is characteristically different from the ‘simple liquid’ structure of Cs (or e.g. Ar) [12] in that the first peak is rather asymmetric, as is the first peak in  $g(r)$  which has a rather pronounced shoulder on the high  $r$  side (see figure 1). This shoulder remains as  $T$  increases, and rather it is the lower  $r$  part of the peak that decreases in intensity. However, in common with Cs, the position of the first peak and minimum in  $g(r)$  are relatively independent of temperature. This indicates that the density decrease does not occur by a uniform expansion, but rather by a decrease in the local average coordination number. In Hg this decrease does not appear to be quite linear with temperature, indicating some change in the interatomic interaction potential, in contrast to Cs which shows a highly linear behaviour [13].

The peak and shoulder in  $g(r)$  for Hg have been interpreted as indicating the existence of metallic and semiconducting local clusters, whose relative proportion then changes as  $T$  increases [6–8]. This idea forms the basis for the analysis of RMC models of expanded liquid Hg, based on the data of Tamura [5], which are described in this paper.

## 2. RMC modelling

The RMC method has been described in detail elsewhere [14], so here we will only provide important details. All models consisted of 4000 atoms in cubic boxes at the appropriate density (which are the same as the experimental values [5]—see table 1), with periodic boundary conditions. Initial RMC modelling of the data at intermediate temperatures produced rather strange  $g(r)$ , particularly when the data was fitted closely. This behaviour could be traced to some small systematic errors, probably in the form of modulations of the data and/or a non-constant background. The fact that there are errors can be seen from the  $g(r)$  obtained by direct Fourier transform (figure 1), which have a definite peak at low  $r$  where they should be zero. Some systematic errors are likely because the experimental technique used by Tamura [5] is rather difficult in any case, and this is only compounded by measuring a difficult material like Hg at high  $T$  and  $P$ . The original data, as well as small corrections for many other effects, have to be divided by the wavelength variation of the intensity of the incident beam and the  $Q$  dependent form factor. Small errors in the former, or in the latter which will in fact change slightly as the density changes, will lead to unwanted modulations in  $S(Q)$ . Background scattering, which is difficult to measure in x-ray experiments, becomes convoluted with this. We would therefore like to stress that although we have identified errors and have to correct for them, as described below, we consider that the data of Tamura [5] is actually of remarkably high quality considering the demands of the experiment.

**Table 1.** Densities and corresponding temperatures for the RMC models of expanded liquid mercury.

$T$ (K)	$\rho$ (g cm <sup>-3</sup> ) [5]	$\rho$ (Å <sup>-3</sup> )
293	13.55	0.0407
523	12.98	0.0390
773	12.40	0.0372
1073	11.57	0.0347
1273	10.98	0.0330
1373	10.66	0.0320
1473	10.26	0.0308
1573	9.81	0.0295
1623	9.53	0.0286
1673	9.25	0.0278
1723	8.78	0.0264
$T_{M-NM}$	~9	~0.027
1773	8.26	0.0248
1803	6.8	0.0198
$T_c$ (1751)	5.8	0.0174

In order to reduce the effect of these errors we have used the following procedure.  $g(r)$  was initially determined using the inverse program MCGR [15], with the constraints that  $g(r) = 0$  for  $r < 2.6$  Å and that the shape of  $g(r)$  peaks is appropriate considering the  $Q$  range of the data. These constraints make it possible to refine a non-constant background; some results are shown in figure 1. We have then used RMC to fit the MCGR derived  $S(Q)$ , rather than the original data. The differences are in fact rather small. This procedure effectively ‘removes’ some of the errors, but there is no way of removing all modulations. However, we do not consider that the remaining errors affect any of our conclusions.

### 3. Results and analysis

The radial distribution functions, as derived from the RMC models, are shown for some of the temperatures in figure 2. As with expanded Cs, the positions of the first peak (at 3.1 Å) and the first minimum (at 4.3 Å) are almost invariant. This indicates that the liquid does not expand uniformly, but rather that the average coordination around each atom decreases. However, it can be seen that the first peak decreases rapidly in comparison to the shoulder at  $\approx 3.5$  Å, giving a ‘cross-over’ point at  $r \approx 3.2$  Å where  $g(r)$  is almost invariant with temperature. We will initially use this point (slightly arbitrarily) to define the change between atoms which are deemed to be metallicly bonded (shorter distances) and covalently bonded (longer distances). Average coordination numbers calculated from the integral of  $g(r)$  up to 3.2 and 4.3 Å are shown in figure 3. The 4.3 Å coordination varies almost linearly with density, as in Cs, but the ‘metallic’ coordination decreases slightly faster at the higher densities, becoming linear below  $\rho \approx 0.033$  Å<sup>-3</sup>. This is rather higher than  $\rho_{M-NM}$  and seems to have no particular physical significance. However, the non-linear behaviour is evidence of some change in bonding. It should be noted that in the linear region the coordination up to 3.2 Å would not extrapolate to the origin.

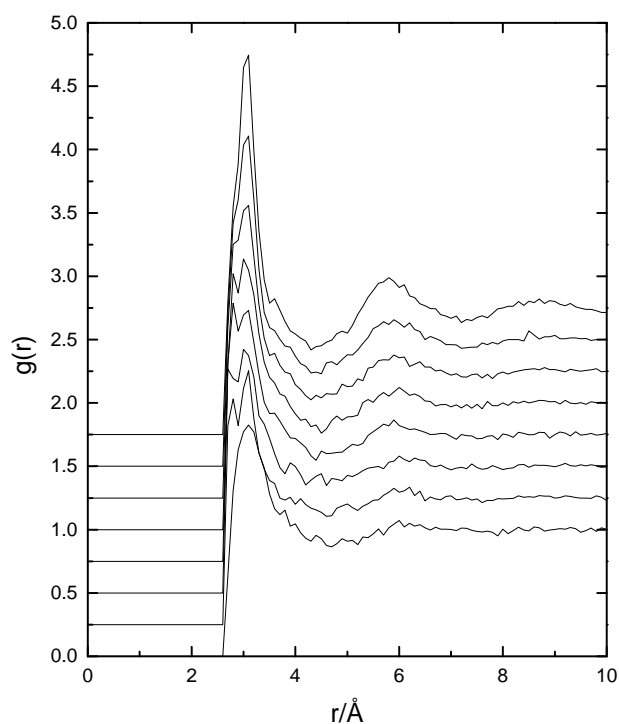


**Figure 2.** Radial distribution function,  $g(r)$ , from the RMC models at (in descending order) 293, 523, 773, 1073, 1273, 1473, 1673 and 1803 K. Consecutive curves are shifted by 0.25 for clarity.

Franz [8] produced model configurations for expanded Hg by removing atoms from a close-packed lattice in order to achieve the required density. The bondlength chosen was 3.1 Å because the mercury dimer has a bondlength of 3.2 Å. She found from electronic calculations that atoms with three-fold coordination or lower had a local gap in the density

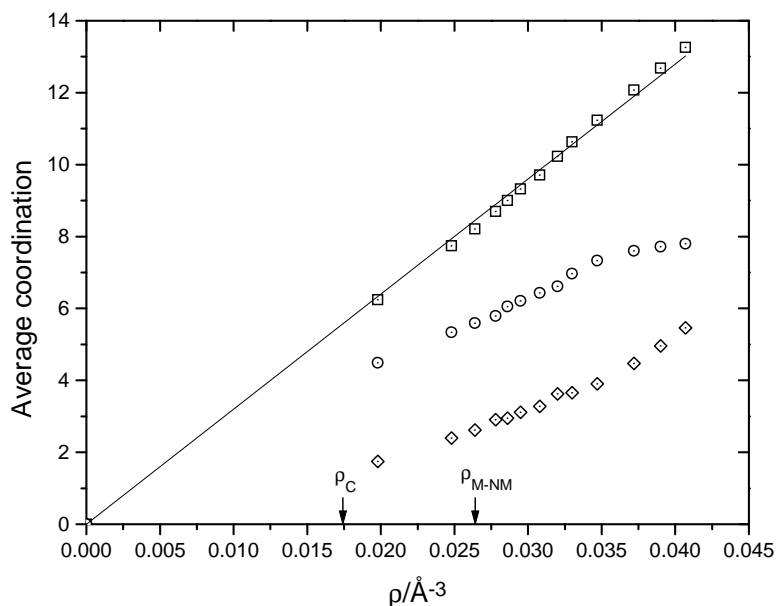


**Figure 3.** Average coordination number obtained from integration of the first peak in  $g(r)$  up to 3.2 Å (diamonds) and 4.3 Å (squares), and the difference (circles). The straight line is a fit to the data for 4.3 Å, constrained to pass through the origin.

of states, and hence could be considered as in a ‘semiconducting’ environment, while those with higher coordination had no local gap and so could be considered as in a metallic environment. Based on this idea, we have divided up atoms within the RMC configurations into those with three-fold coordination within 3.2 Å (which seems to be slightly more appropriate based on the data) and those with higher coordination. We will designate the former as ‘semiconducting’ (s) and the latter as ‘metallic’ (m). The partial radial distribution functions  $g_{mm}(r)$  and  $g_{ss}(r)$  for these ‘species’ are shown in figure 4. Although the definitions of m and s atoms are made based on coordination within the same distance (3.2 Å), it can be seen (figure 4) that  $g_{mm}(r)$  peaks at 3.1 Å while  $g_{ss}(r)$  peaks at 3.5 Å, the same distance as the previously identified shoulder on the first peak in  $g(r)$ . This means that the definitions of metallic and semiconducting atoms based on the peak and shoulder in  $g(r)$ , or coordination number up to 3.2 Å, are in fact highly compatible. We can therefore conclude that atoms in a metallic environment tend to have a higher number of neighbours (four or more) at a relatively short distance, while those in a semiconducting environment have a small number of neighbours at a slightly larger distance. This is of course entirely consistent with what is known about typical metallic and semiconducting structures in the crystalline state. Further support for this comes from the bond angle distributions shown in figure 5 (bonds are defined to neighbours within 3.2 Å).  $P_{mmm}$  has the characteristic shape of a close-packed ‘simple liquid’ [12], with a main peak at 60° and a broader peak at 120°.  $P_{sss}$  peaks at a larger angle,  $\approx 70^\circ$ , indicating a slightly more open local structure, again characteristic of a trend towards covalency. Peak positions in both distributions remain the same as  $T$  increases.

The partial structure factors are shown in figure 6. At high density  $A_{mm}(Q)$  is flat at low  $Q$  but  $A_{ss}(Q)$  shows a steep rise, indicating that semiconducting atoms tend to form small clusters. This is, of course, an almost necessary result of the tendency to have

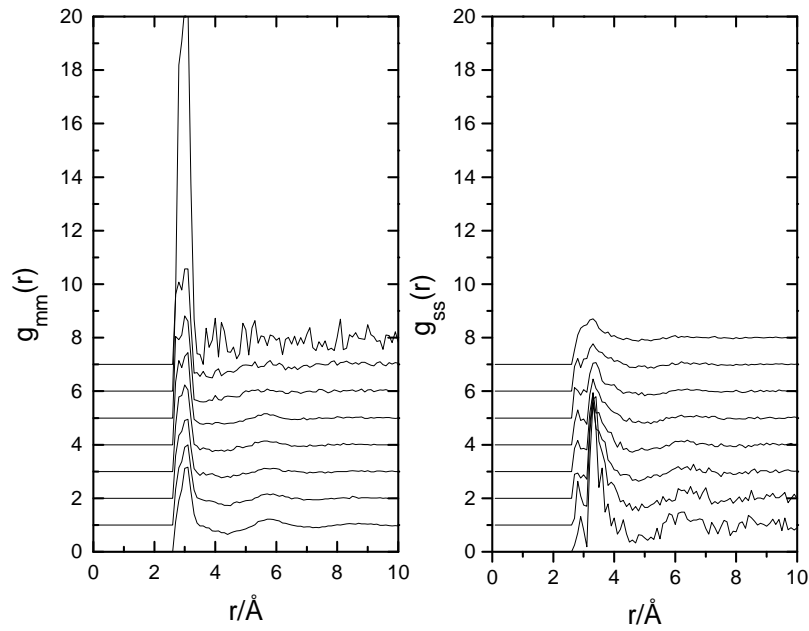


**Figure 4.** Partial radial distribution functions,  $g_{ij}(r)$ , for metallic (m) and semiconducting (s) atoms, as defined in the text, at (in ascending order) 293, 523, 773, 1073, 1273, 1473, 1673 and 1803 K. Consecutive curves are shifted by 1 for clarity.

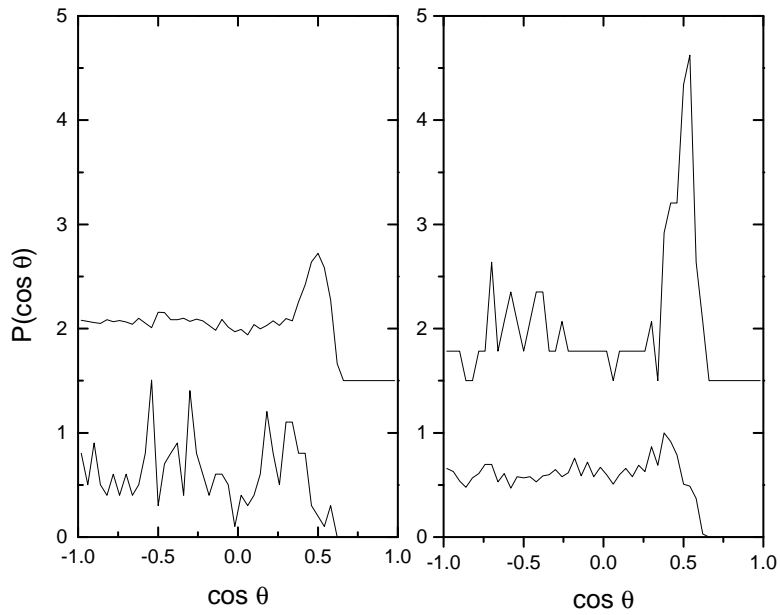


**Figure 5.** Bond angle distribution functions  $P_{ijk}(\cos\theta)$ , for triplets of metallic (top) and semiconducting (bottom) atoms at 1073 K (left) and 1803 K (right).

few neighbours with a more open local structure. Conversely, at low densities  $A_{ss}(Q)$  is flat at low  $Q$  and  $A_{mm}(Q)$  has a steep rise, so metallic atoms cluster within a mainly

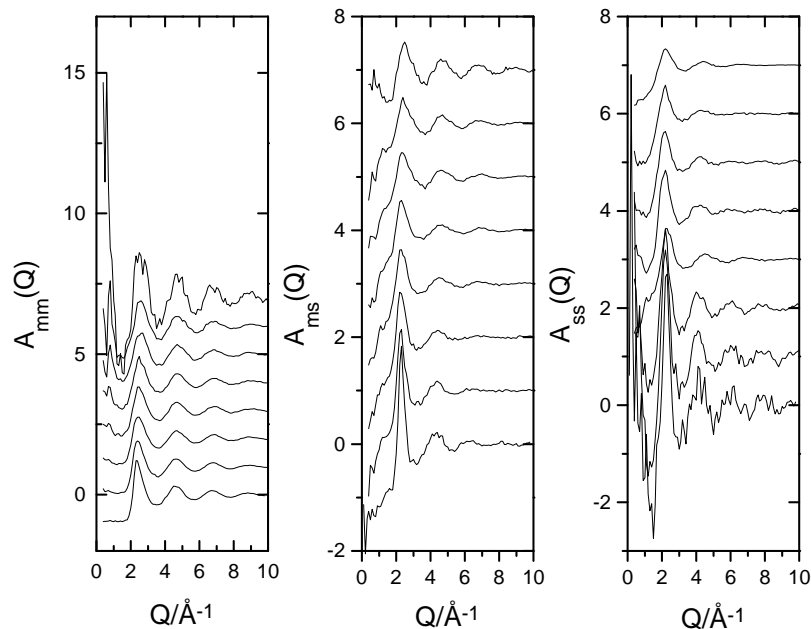


**Figure 6.** Partial structure factors,  $A_{ij}(Q)$ , for metallic (m) and semiconducting (s) atoms, as defined in the text, at (in ascending order) 293, 523, 773, 1073, 1273, 1473, 1673 and 1803 K. Consecutive curves are shifted by 1 for clarity.

semiconducting network. It is interesting to note that at the lowest density  $A_{ms}(Q)$  has the typical shape of an ionic (i.e. charge ordered) liquid [16], with a characteristic ‘Coulomb dip’ at  $Q = 1.5 \text{ \AA}^{-1}$ . ‘Ball and stick’ pictures of sections of some of the RMC configurations are shown in figure 7. Here we have drawn s atoms as ‘balls’ and bonds between m atoms (i.e. within  $3.2 \text{ \AA}$ ) as ‘sticks’. The features described above can be seen quite clearly.

In expanded Cs we were able to show that the M–NM transition could be characterized as a percolation transition in the network of metallic bonds [9, 11]. In the present case a similar analysis is slightly more difficult, since the transition is not so sharp (being metal–semiconducting rather than metal–insulator) and it does not occur close to the critical point. If we include all atoms then the bond network (up to  $3.2 \text{ \AA}$ ) has a percolation transition between  $0.0248 \text{ \AA}^{-3}$  and  $0.0198 \text{ \AA}^{-3}$ , which is below  $\rho_{M-NM}$  and above  $\rho_c$ . However, using the definition of m and s atoms based on coordination number given above, we find a percolation transition in the metallic bond network between  $0.0295 \text{ \AA}^{-3}$  and  $0.0286 \text{ \AA}^{-3}$ , which is reasonably consistent with the experimental value of  $0.027 \text{ \AA}^{-3}$  for  $\rho_{M-NM}$ . It should be noted that in any case the experimental determination of this value is not particularly precise. In figure 8 we show the coordination number distribution of all atoms up to  $3.2 \text{ \AA}$ . At the lowest density, as  $\rho_c$  is approached, there is a sharp rise in the number of atoms with onefold coordination, i.e. mainly dimers. For the purposes of this paper we will define dimers/trimers as groups of two/three m atoms which do not have any other m atoms as neighbours; for example, a chain of three m atoms is a trimer, even though it contains two onefold coordinated and one twofold coordinated m atoms. Figure 9 shows the percentage of m and s atoms as a function of density. It can be seen that the critical point coincides very closely with the density at which the number of m atoms extrapolates to zero. In figure 6 it can be seen that at the lowest density the entire low  $Q$  rise in  $S(Q)$



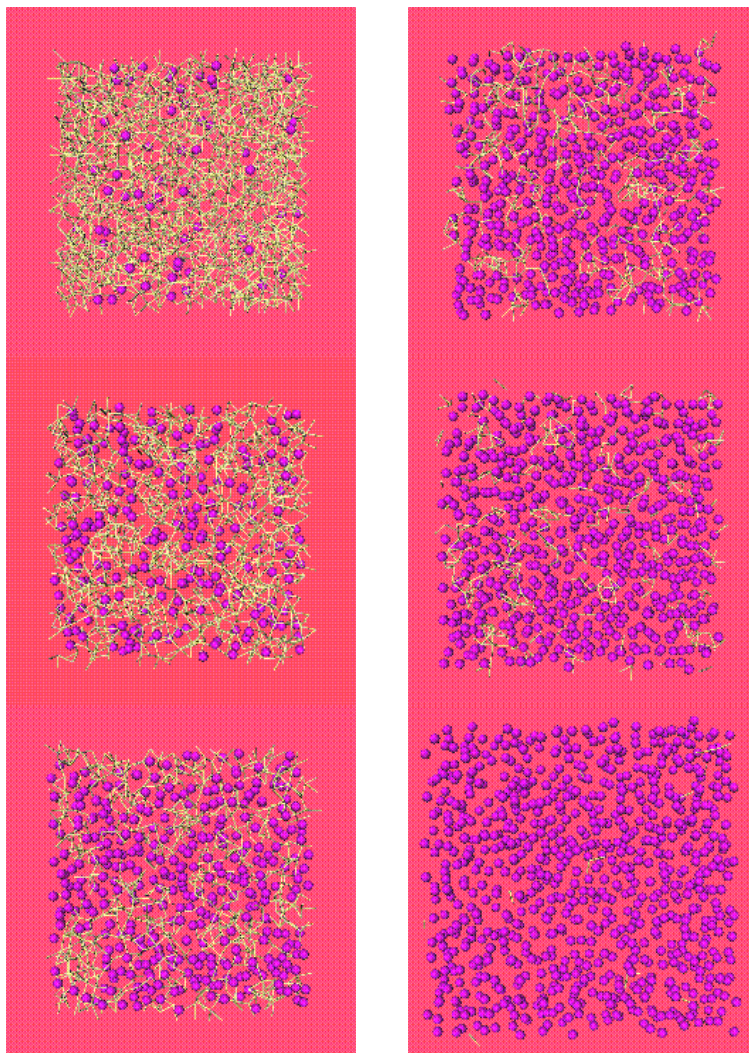


**Figure 7.** 10 Å thick sections of configurations for expanded Hg at 293, 773, 1073, 1473, 1673 and 1803 K (top left to bottom right). Semiconducting atoms and metallic bonds, as defined in the text, are drawn as balls and sticks, respectively.

(which is necessary because of the divergence of the compressibility at the critical point) is due to  $A_{mm}(Q)$ ;  $A_{ss}(Q)$  remains flat at low  $Q$ . Both of these features suggest that as  $\rho_c$  is approached the structure may be characterized as consisting of relatively isolated metallic clusters within a more uniform semiconducting network—although this network is gradually breaking up into low coordination clusters, for example dimers and trimers.

Franz [8] has determined the M–NM transition as a percolation transition of the ‘local gap’ corresponding to the s atom network, i.e. when the gap becomes delocalized. In her case this is similar to the point where the metallic network ceases to percolate because the atoms occupy positions on a close-packed lattice (the density is decreased by removing atoms without any change in atomic positions). For a disordered structure (as in our case)

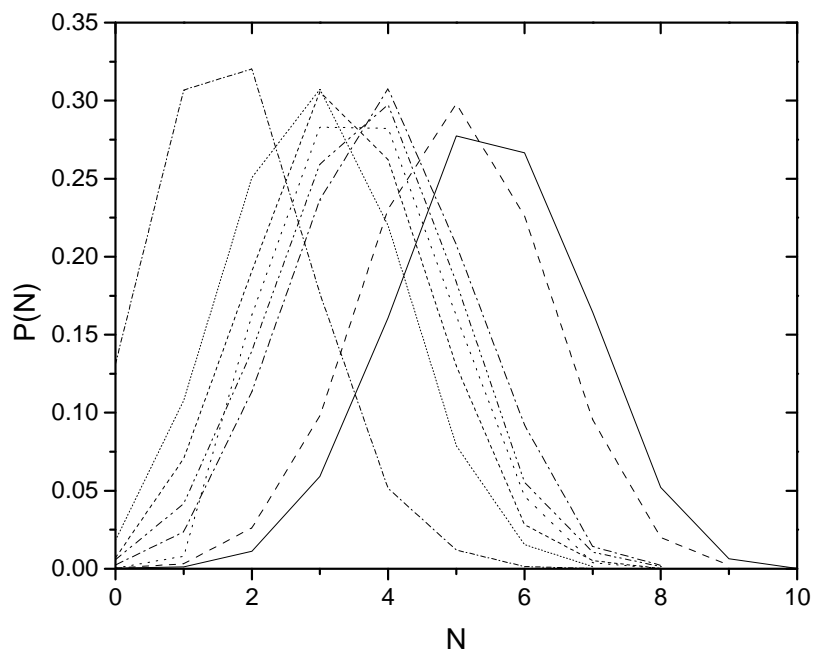


**Figure 8.** Coordination number distributions for neighbours within  $3.2 \text{ \AA}$  at 293 (solid curve), 523 (dashed curve), 773 (dotted curve), 1073 (dash-dotted curve), 1273 (dash-dot-dotted curve), 1473 (short dashed curve), 1673 (short dotted curve) and 1803 K (short dash-dotted curve).

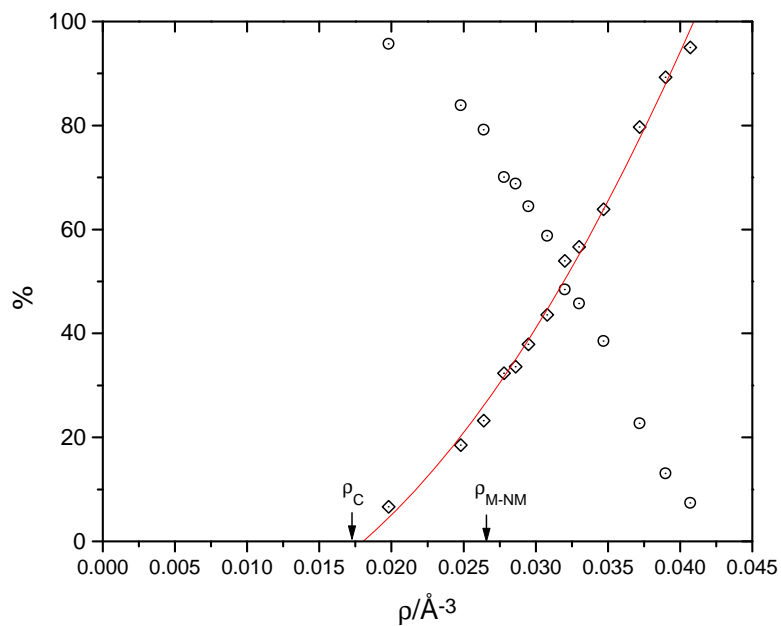


**Figure 9.** Percentages of m (diamonds) and s (circles) atoms as a function of density. The full curve is a polynomial fit to the m atom data.

it would be possible to have a situation where both m and s networks were percolating at the same time, which would be 'metallic'. We have therefore considered that a definition

based on the percolation transition of the metallic bond network is more appropriate.

It is interesting to note that the ratio of the m atom density at the M–NM transition to that at the triple point is  $\sim 0.19$ , which is very similar to the value of 0.21 for expanded Cs [11], despite the fact that for Cs  $T_{M-NM}$  coincides with  $T_c$  while in Hg they are significantly different.

#### 4. Conclusions

The structure of liquid Hg at any instant may be considered as consisting of interpenetrating networks of atoms which have either predominantly metallic bonding, i.e. electrons are delocalized, or predominantly semiconducting bonding, i.e. electrons are localized. Consistent evidence for this is obtained from the change of  $g(r)$  with temperature, the bond angle distribution and the distribution of atoms with lower and higher coordination numbers. Individual atoms change between different regions because of the natural fluctuations due to temperature. At low temperature metallic regions dominate, so liquid Hg is a metal, and the semiconducting regions are microphase separated within the metallic network. As  $T$  increases and density decreases, the reduction in local coordination number is achieved mainly by decrease in the number of metallic bonds. At about 1600 K (along the co-existence curve) this metallic bond network passes through a percolation transition and ceases to be fully interconnected. This is close to the metal–non-metal transition point as defined from experiment. The structure then consists of clusters of metallic atoms within a semiconducting network. The critical point may be related to the complete disappearance of metallic clusters.

#### Acknowledgment

We thank Professor Tamura for provision of the numerical structure factors.

#### References

- [1] Schmulzler R W and Hensel F 1972 *Ber. Bunsenges Phys. Chem.* **76** 53
- [2] El-Hanny U and Warren W W Jr 1975 *Phys. Rev. Lett.* **34** 1276
- [3] Schönherr G, Schmulzler R W and Hensel F 1979 *Phil. Mag.* B **40** 411
- [4] Yao M and Endo H 1982 *J. Phys. Soc. Japan* **51** 966
- [5] Tamura K 1994 *Z. Phys. Chem. Bd.* **184** S 85
- [6] Cohen M H and Jortner J 1994 *Phys. Rev. Lett.* **30** 699
- [7] Mattheiss L F and Warren W W Jr 1977 *Phys. Rev. B* **16** 624
- [8] Franz J R 1986 *Phys. Rev. Lett.* **57** 889
- [9] Nield V M, Howe M A and McGreevy R L 1991 *J. Phys.: Condens. Matter* **3** 7519
- [10] Arai T and McGreevy R L 1996 *Phys. Chem. Liq.* **33** 199
- [11] Arai T and McGreevy R L 1998 *Phys. Chem. Liq.* at press
- [12] Howe M A, McGreevy R L, Pusztai L and Borzsak I 1993 *Phys. Chem. Liq.* **25** 204
- [13] Winter R and Hensel F 1989 *Phys. Chem. Liq.* **20** 1
- [14] McGreevy R L 1992 *Ann. Rev. Mater. Sci.* **22** 217
- [15] Pusztai L and McGreevy R L 1998 *Phys. Scr.* submitted
- [16] Edwards F G, Enderby J E, Howe R A and Page D I 1975 *J. Phys. C: Solid State Phys.* **8** 3483